AUTHOR ACCEPTED MANUSCRIPT

Analysis of the Relationship Between Hip Joint Flexion/Extension and Torques in the Mark III Space Suit using a Computational Dynamics Model

Patrick McKeen[a], Conor Cullinane[b], Richard Rhodes[c], and Leia Stirling[d,*]

[a]Aeronautics and Astronautics Department, MIT.

[b]Health Sciences and Technology Program, the Aeronautics and Astronautics Department at the Massachusetts Institute of Technology (MIT) and Harvard Medical School, Cambridge, MA.

[c]Advanced Pressure Garment Technology Development Lab, the Crew Survival and Space Suit Systems Branch EC5, NASA, Johnson Space Center.

[d]Department of Industrial and Operations Engineering, Robotics Institute, University of Michigan.

[*]Corresponding author: Leia Stirling, leias@umich.edu.

Accepted 17 November 2020. Published online 18 December 2020.

Published article: McKeen, P., Cullinane, C., Rhodes, R., & Stirling, L. (2021). *Computer Methods in Biomechanics and Biomedical Engineering*, 24(8), 831–843. doi:10.1080/10255842.2020.1853708

This author accepted manuscript has been reformatted for readability. Pagination differs from the published article.

Abstract

Advanced SSAs (e.g., the Mark III (MKIII)) were designed to increase mobility by eliminating the volume change associated with bending joints by using constant-volume rigid components with bearings connecting these components. Even with these changes, there are added torques required by the operator to drive the motion, which increases the energy expenditure with respect to unsuited motion. Part of the added effort stems from the mass and inertia of the suit, as well as frictional resistances to motion. This research considers the relationship between joint torques that an operator must generate and the resulting flexion/extension of the hip bearing assembly. A computational dynamics model of the MKIII inclusive of inertial and bearing friction properties was created and sensitivities of the model to input parameters (e.g., applied force, direction of gravity, bearing friction magnitude, knee angle) were investigated. The model was configured to match previously collected benchtop experimental suit data without a human that was externally forced. The model captured the hysteretic behaviour and estimated about 80% of the mean hip angle range as compared to the experimental data. Decreasing bearing resistance increased alignment with the experimental data. The torque due to inertia and friction each had periods where they dominated the total torque, supporting the importance of minimizing both mass and bearing friction. The present effort also highlighted how external forces and boundary conditions affected peak hip flexion/extension. Future efforts can use these types of dynamics models to examine motions driven internally by a person to achieve specific motions.

Keywords: bearings; dynamics, joint torque, kinematics, motion envelope

Introduction

Extravehicular activity (EVA) space suits ("space suits" or "suits") have been used from the beginning of human spaceflight through the modern day to provide life support and protect the astronaut. The design of these critical tools and their constituent space suit assemblies (SSAs) has many aspects: spacesuit designs must consider the interaction of mass, volume, walking effort, mobility, agility, and suit fit (Abramov, Moiseyev, & Stoklitsky, 2001). Operators wearing earlier EVA suits have developed a variety of injuries in a range of locations, including the shoulder and hip, due to prolonged use, including

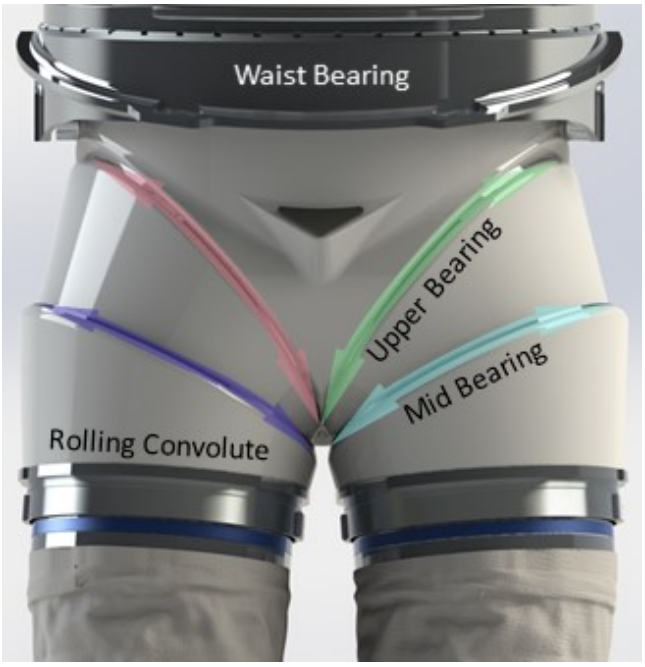


Figure 1. The Mark III (MKIII) Computer Aided Design (CAD) model showing the hip brief assembly (HBA) mobility unit. The depiction of the MKIII suit in this figure was generated from the kinematics model of the suit that was used to compare operator and suit ranges of motion (ROMs) (Cullinane et al., 2017b).

erythema, abrasions, muscle soreness/fatigue, paresthesia, bruising, blanching, and edema (Opperman, Waldie, Natapoff, Newman, & Jones, 2010; Scheuring, Mathers, Jones, & Wear, 2009; Stirling, Arezes, & Anderson, 2019). To address these difficulties, a good design should maximize human performance and efficiency, while preventing injury (Gernhardt et al., 2009).

The suit's ability to meet these criteria depends heavily on the design choices. For example, many suits use flexible limbs that generate "springback" forces due to volumetric changes (Hoffman, 2004; Newman, Schmidt, Rahn, Badler, & Metaxas, 2000; Schmidt & Newman, 2001). These springback forces can reduce mobility and increase energy usage for the suit occupant (Chappell et al., 2017), impacting lower limb movements. Apollo astronauts reported difficulty with locomotion and exertion in their thighs to the point of fatigue (Chullen et al., 2013; Scheuring et al., 2008). Such extensive use of the thigh was likely connected to motions of the hip used for walking, indicating the suit hip joint and the gait motion may be particularly susceptible to springback forces (Graziosi & Ferl, 1999; Wickman & Luna, 1996).

Advanced SSAs, such as the Mark III (MKIII), were designed to reduce this problem and increase mobility by eliminating the change in volume associated with bending some joints. To do so, the MKIII uses constant-volume rigid components and the degrees of freedom (DOFs) of the relevant joints are captured by bearings connecting these components (Flugel, Kosmo, & Rayfield, 1984; Kosmo, Spenny, Gray, & Spampinato, 1988). This approach is most clear in the MKIII"s hip bearing assembly (HBA), shown in Figure 1. The HBA mobility is comprised of several bearings. The upper and mid bearings of the HBA provide hip flexion/extension and adduction/abduction. The rolling convolute joint has a bearing that provides rotation for internal and external rotation of each leg, but also a pivot point that provides additional adduction/abduction. Together, these joints allow the hip of the occupant a rather large motion envelope (Cowley, Margerum, Hharvill, & Rajulu, 2012).

Despite this envelope and its constant volume, the HBA is susceptible to other mobility issues which can restrict the occupant (Cowley et al., 2012; Norcross et al., 2010). The suit operator's motion is bounded by the geometry and placement of the bearings (Kosmo et al., 1988). If these bounds are misaligned with the

occupant's natural motions, they are forced to use new and unnatural "programmed" motions (Abramov et al., 2001; Cullinane, Rhodes, & Stirling, 2017b). Improving the alignment of natural motions and the suited ROM could reduce the use of programmed motions and thus improve mobility, as previous work by McKeen & Stirling (McKeen & Stirling, 2020) have considered. In addition to the geometric limits, there are added torques required by the operator to drive the motion. Part of the added effort stems from the added mass and inertia of the suit—the occupant is moving not only their limbs, but the added weight of suit components. However, the suit also has frictional resistances to motion. The necessary hip torques, for example, provided by the occupant to move the MKIII HBA are related to the angular velocity of the joint due to the friction inside the bearings (Cullinane, Rhodes, & Stirling, 2015). The nature and magnitude of the added forces and torques that the suit requires from an occupant govern the impact that the suit has on occupant mobility. Understanding the relationship between these joint torques and suit motion will inform suit designers, mission planners, and crewmembers, allowing them to improve mobility for occupants. This relationship can be used to help improve utilization of the current suit design, allow for more efficient and effective crewmember training, and help inform future designs. Specifically, this information could help increase mobility and reduce deviations from natural motions, allowing injury risk and metabolic cost to be reduced (Wehner et al., 2013), and extending exploration capabilities.

This understanding of required torques and their relationship to suit motion could allow engineers to predict human-suit interactions before a prototype is manufactured. The predictions can be used to make design changes prior to fabrication, reducing costs and allowing a larger design space to be considered, which can lead to a more optimized final design. A dynamics model can be used to capture the interaction between torques and suit motion. Such a model is also useful for supplementing experimental suit analyses and can allow for more operationally relevant analyses than are possible experimentally due to sensing difficulties and volume constraints.

In this research, we create and apply a computational dynamics model of the MKIII, specifically considering the required HBA joint torques that an operator must generate to achieve flexion/extension of the hip. In this paper, we first present the model development and validation methods. We then use this model to investigate the component-level contributions to overall motion and torques, including the relative significance of inertial and frictional resistances. Finally, we perform a sensitivity analysis to understand the influence that force profile, component mass, bearing resistances, and gravity have on the joint torques.

Methods

Model Development

The SolidWorks (Dassult Systems S.A., Vélizy, France) rigid-body model developed and applied previously (Cullinane et al., 2017b) was extended from a kinematics model to enable analysis of the dynamics. This model contained the geometry of each component, and the constraints that restrict their motion with respect to one another. Thus, this model already encompassed the DOFs of each component. The properties added were the mass and inertia properties for each component and the resistance profiles to account for the friction in each bearing.

While the exact inertia properties of each component were not known, the geometry of the components were. The components were weighed individually and the material densities of each component were assigned to match these experimental weights of the components of the MKIII. The associated inertial properties were calculated from the part geometries and masses, as part of SolidWorks dynamics calculations and component properties.

To understand the friction inside the model, the resistance profiles of each bearing were needed. Cullinane et al. (Cullinane et al., 2015) characterized the torque required to rotate the HBA upper and mid

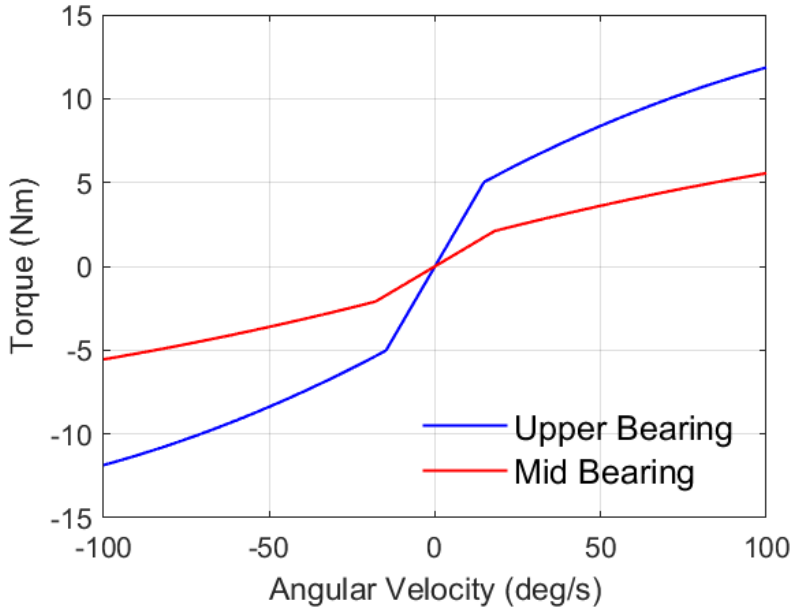


Figure 2. The resistance torque curves used in the model as a function of angular velocity.

bearings for a range of angular velocities and found a speed dependent relationship. To understand the bearing resistances, combined bearing torque and angular velocity data (Cullinane et al., 2015) were averaged over trial (360 degree rotations of the bearing) and rotational sense (clockwise vs. counter-clockwise). Separate polynomial fits of these torques were created for both the upper and mid bearings, shown respectively in Equations 1 and 2, and plotted in Figure 2. These frictional forces were added to the SolidWorks simulation as reaction torques. The resistance torque magnitude was calculated using the instantaneous angular velocity of the bearing and applied (in the direction opposite to the angular velocity) at each time step of the simulation between the components connected by the bearing. Additionally, the bearing at the rolling convolute joint, which was not characterized in Cullinane et al. (Cullinane et al., 2015), was modelled as having a simple linear frictional torque, with a damping constant of 0.1 $\mathrm{Nm}/(\mathrm{deg/s})$.

Proximal / Upper Bearing Resistance Torque Equation:

$$\tau_{\mathrm{upper}}(\omega) = \begin{cases} \left(0.33958\,\dfrac{\mathrm{Nm}}{^\circ/\mathrm{s}}\right)|\omega|, & |\omega| < 14.8\,^\circ/\mathrm{s}, \\ \left(-0.0003\,\dfrac{\mathrm{Nm}}{(^\circ/\mathrm{s})^2}\right)|\omega|^2 & \\ \quad + \left(0.1146\,\dfrac{\mathrm{Nm}}{^\circ/\mathrm{s}}\right)|\omega| + 3.3958\,\mathrm{Nm}, & |\omega| \geq 14.8\,^\circ/\mathrm{s}. \end{cases} \tag{1}$$

Distal / Mid Bearing Resistance Torque Equation:

$$\tau_{\mathrm{mid}}(\omega) = \begin{cases} \left(0.11711\,\dfrac{\mathrm{Nm}}{^\circ/\mathrm{s}}\right)|\omega|, & |\omega| < 18.0\,^\circ/\mathrm{s}, \\ \left(-0.0001\,\dfrac{\mathrm{Nm}}{(^\circ/\mathrm{s})^2}\right)|\omega|^2 & \\ \quad + \left(0.0538\,\dfrac{\mathrm{Nm}}{^\circ/\mathrm{s}}\right)|\omega| + 1.1711\,\mathrm{Nm}, & |\omega| \geq 18.0\,^\circ/\mathrm{s}. \end{cases} \tag{2}$$

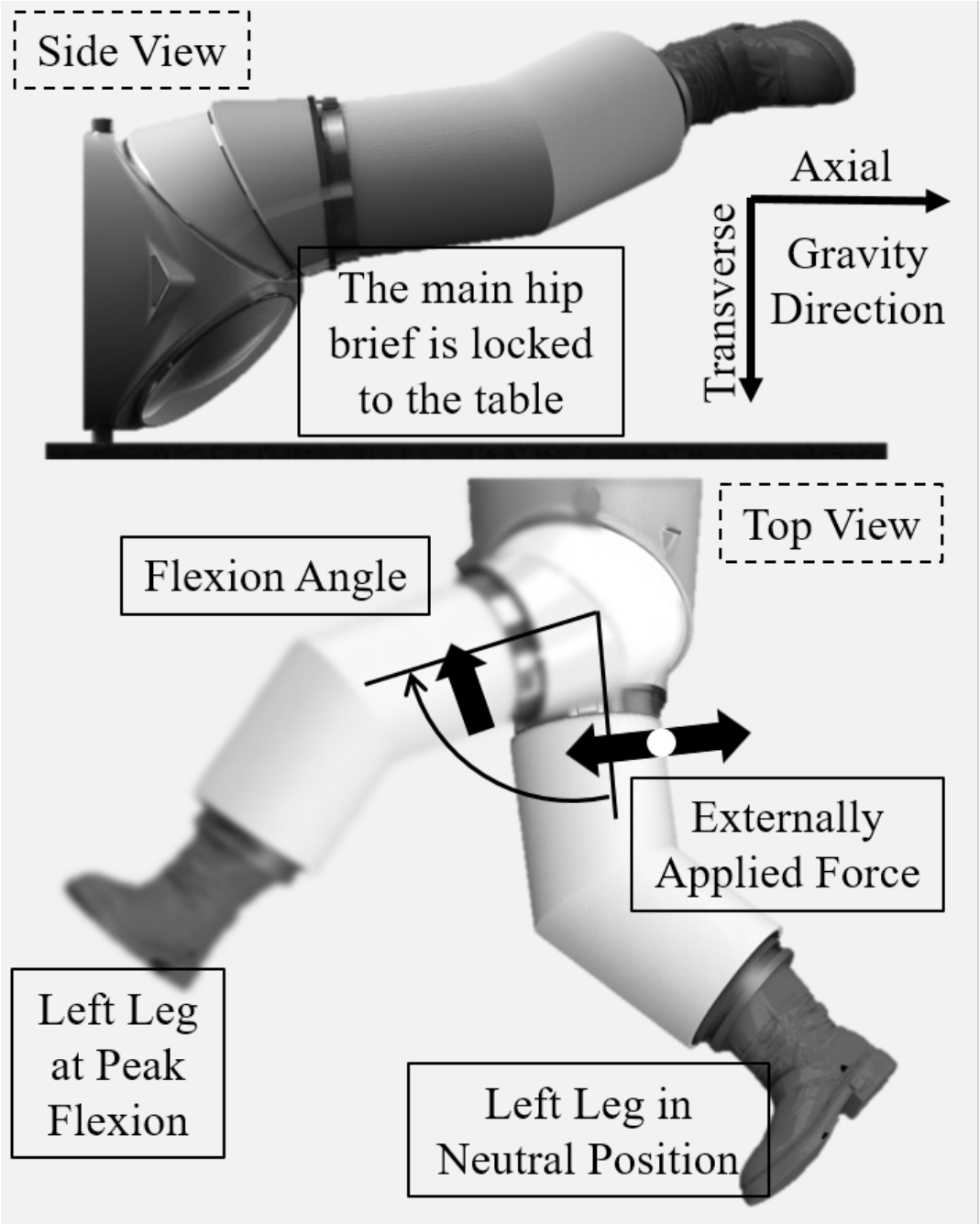


Figure 3. The SolidWorks Motion Analysis rigid-body dynamics model was implemented to resemble the experimental analyses performed at Johnson Space Center (JSC). The "Top View" depicts the left leg in the neutral, starting position, as well as at peak flexion angle. The right leg was stationary and fixed to the table and is not shown.

Motion was simulated within SolidWorks using the embedded Motion Analysis (MA), which treats each component as a rigid body, with the assembly mates defining the constraints on their relative motion. During the runs of the simulation, MA uses its built-in variable-time-step dynamics solver to determine the forward dynamics solution of the assembly. By running the simulation with varying boundary conditions, assembly properties, and applied forces, the behaviour of the MKIII in various situations can be tested.

Validation

The model, including the HBA, soft goods, and boot, was validated against experimental data from Valish and Eversly (Valish & Eversley, 2012). The original experimental study, performed on the MKIII SSA at NASA Johnson Space Center (JSC), focused on the left leg of an unmanned suit. The right leg and waist bearing were strapped horizontally to a table, isolating the motion on the left side of the HBA and left leg. The test operator then applied an external oscillating force (forcing the limb between flexion and extension) just distal to the rolling convolute joint, while manually supporting the boot with their contralateral hand. The magnitude of the oscillating force was collected at 2.9 Hz, while joint angles were estimated with an inertial measurement unit.

MotionAnalysis was performed with the computational model aligned to mimic the experimental setup in the NASA JSC experiments (Valish & Eversley, 2012). These boundary conditions were matched computationally by orienting the suit model horizontally, setting gravity to 1g downwards, and removing the right limb and everything above the waist bearing, while locking the main hip brief in place (Fig. 3). This limited the motion to the HBA and the left side's rolling convolute joint, lower-leg soft good, ankle flange, and boot. The computational model was then forced externally, just distal to the rolling convolute. The force was applied orthogonal to the rolling convolute to mimic the experiment as closely as possible. The instantaneous hip angles were calculated from a vector defined from a virtual hip joint center (located at the centroid of the upper bearing) and the centroid of the rolling convolute at each time step. Since the programmed motion of the HBA forces the flexion/extension to have an out-of-plane component, the flexion/extension angle was taken as the projection of that motion on the sagittal plane.

Matching the computational model to a pre-existing experiment created several challenges. While they are discussed further in the discussion section, these challenges, and the manner with which they were dealt, are worth noting here. During the experiment at JSC, the knee was not locked into a fixed position and was free to rotate in flexion/ extension. The orientation of the knee was not recorded and could not be used as an input to the computational model. Although the experimental setup allowed for knee motion, the computational model used a rigid body soft goods leg, which was segmented into two parts with an artificial knee joint added. The modelled knee joint was fixed during each MotionAnalysis. Based on observations of the experimental videos, a knee flexion angle of 45 degrees was nominally selected (Fig. 3).

Similar to the unrecorded knee data, there were forces in the experiment of which we do not have measurements. For example, video recordings of the experiment show operators bending their wrists, potentially changing the direction of their applied force. However, the load cell used to record the force only recorded the normal component, so there was no data about any potential off-axis forces. Due to the absence of concrete data, these forces were neglected in the model—the possible impact of this decision is discussed later in the paper. Additional forces could also arise from the manual support of the boot. The magnitude of the operator's vertical support on the boot was not quantified or recorded and could not be imitated. Thus, the computational model did not apply a force to the boot, but rather stipulated motion constraints in MotionAnalysis, setting a minimum distance the boot must maintain from the surface of the table.

Sensitivity Analyses

This model was developed to understand how the force/torque environment relates to motion of the suit. To analyze the factors which most contributed to the required joint torques, we performed a sensitivity analysis on the model. Specifically, five aspects of the model were modified: (1) external force profile (nominal: experimental, sinusoidal), (2) bearing resistance (50%, nominal: 100%, 150%), (3) boot mass

(nominal: 1.08 lbs, 1.55 lbs, 1.73 lbs), (4) gravity magnitude (Lunar, Martian, nominal: Earth), and (5) gravity direction (nominal: transverse, axial).

These aspects were selected for several reasons. The experimental forcing function was human-driven and experimentally recorded, and thus had variance from experimental noise and human variability. The sinusoidal force profile used in sensitivity analysis was a simple sinusoid, with the frequency and magnitude were selected to match the peaks of the experimental data, serving as a "cleaner" version of the force profile so the effect of that variance could be investigated. The other variations used in the sensitivity analysis (bearing friction, boot mass, and gravity direction and magnitude) were considered to understand the relative significance of friction (bearing resistance) versus inertial effects (gravity and boot mass) on required hip torques and the force/torque environment. Additionally, these analyses were chosen to grant insight into how hip torques and the force/torque environment could vary between the experimental and operational conditions, such as if larger boots were used, if gravity was oriented axially (as in a standing astronaut), or if the suits were used off-planet with less gravity. In the cases modifying the magnitude of gravity, the applied force was scaled to 37.5% of its magnitude (See Table I). This change was introduced to prevent the limb being driven outside its operational range in the lower gravity environments, and the specific value was chosen experimentally.

A total of 14 cases were examined (Table I). Each of the modified cases was compared to a nominal base case that was most relevant to the case under consideration (highlighted in Table I). In addition to the qualitative comparisons based on the shape of motion and hysteresis, the peak flexion and extension angles were compared, also shown in the Table. The statistical comparison was made using a 2-sample T-test, while assuming different variance. Standard deviations were compared using an F-Test. The significance level used was 5% ($\alpha = 0.05$). To remove transient effects, the first hysteresis loop was removed in each case, leaving 8 samples of flexion and 7 samples of extension for analysis.

Torque Decomposition

The computational model was also used to determine the relative significance of inertia and friction, in terms of their impact on required hip joint torque. Another MotionAnalysis was performed—this trial used the sinusoidal forcing function to remove the human-induced variability. All other components of the model, including those modified in the sensitivity analysis (boot mass, bearing resistances, gravity magnitude, and gravity direction), were left in their nominal configurations.

For the decomposition, the frictional bearing torques were calculated from bearing angular velocity, using the same polynomials which were used to define the resistance torques (see Equations 1 & 2). The absolute values were used to avoid torques in opposite directions cancelling each other out and to capture the dissipative nature of the frictional resistance. The torque derived from the boundary conditions and table mount were not considered. The difference between the total applied torque from the MotionAnalysis and the estimated frictional bearing torques can be attributed to inertial effects (inclusive of gravity).

Results

Validation

The experimental data and computational model results are shown in Fig. 4 and summarized in Table I. The nominal model (Case 2) consistently under-estimated the experimental model (Case 1) hip angle during peak flexion ($p<0.001$), but was not significantly different for peak extension ($p=0.194$).

The model estimates about 80% of the mean hip angle range as compared to the experimental data and captures the hysteresis appropriately. Although there is a consistent statistical difference in peak flexion,

Table I. Comparison of Experimental and Computational Results

Case configurations

Case	Bearing resistances	Boot size (lbs)	Forcing function	Gravity level	Gravity direction
1	Experiment	N/A	Exp	Earth	Transverse
2	Nominal	1.08	Exp	Earth	Transverse

Hip angles

	Peak flexion (8 cycles)					Peak extension (7 cycles)				
Case	Max (deg)	Min (deg)	Mean (deg)	Std (deg)	p	Max (deg)	Min (deg)	Mean (deg)	Std (deg)	p
1	77.70	58.88	69.46	6.82	<0.001	-41.96	-30.26	-35.54	4.07	0.194
2	51.62	49.22	50.65	0.93	-	-35.12	-32.08	-33.29	1.03	-

The case numbers down the far left column indicate different configurations. Case 1 represents the results from experimental analysis, while Case 2 corresponds to the results from the SolidWorks Motion Analysis model in its nominal confiugration.

operationally the model is a reasonable approximation of the overall motion characteristics and response of the SSA to an external forcing.

Sensitivity Analyses

The 14 Cases used in the Sensitivity Analyses, each with a varied model input, are defined and their respective results collated in Table II.

In Case 3, which used a sinusoidal forcing function with less variation than the experimentally recorded force, there was reduced variability in peak flexion and extension (Fig. 4a). Specifically, the sinusoidal input resulted in smaller standard deviations for both flexion ($F(7,7) = 52.04$, $p<0.001$) and extension ($F(6,6) = 341.75$, $p<0.001$).

Variations in bearing resistance (Cases 6 and 7 in Fig. 4b) resulted in differences when compared to the nominal model (Case 2). Increasing the bearing resistances results in a decrease in hip flexion and extension, while decreasing the bearing resistances results in an increase in hip flexion and extension.

Changing the boot masses (Cases 4 and 5) from the nominal configuration (Case 2) did not significantly affect peak flexion (Fig. 4c), although did significantly affect extension ($p=0.029$ and 0.012, respectively).

When the direction of gravity is in the axial direction, as in Case 8, the hip flexion and extension angles are reduced compared to the transverse (nominal) direction, (Fig. 5a). In Figures 5b and 5c, it can be seen that reducing gravity results in increases in hip flexion and extension angles. This is true both when gravity is oriented transversely (Cases 9, 10, and 11) and axially (Cases 12, 13, and 14).

As can be observed in Figures 4 and 5, there is a consistent hysteresis across all tests. While most evident in Case 3 (with the cleaner sinusoidal forcing function), the size and shape of the hysteresis is similar in all cases, when compared to their reference baseline.

To further understand the source of this hysteresis, Figure 6 presents the underlying bearing motion for one flexion/extension cycle from Case 3, relative to the hip flexion/extension. As can be seen in Figure 6a, the upper bearing is rotating more than the mid bearing during hip flexion (0-20% and 60-100% of the cycle), but the mid bearing is rotating more in hip extension (20-60% of the cycle). Figure 6b highlights that the bearings are frequently moving in opposite directions. The opposing motion happens throughout the cycle, but is most apparent from 0-25% and 50-90% of the cycle.

Table II. Computational Results used in Sensitivity Analysis

Case configurations

Case	Bearing resistances	Boot size (lbs)	Forcing function	Gravity level	Gravity direction
2	Nominal	1.08	Exp	Earth	Transverse
3	Nominal	1.08	**Sinusoidal**	Earth	Transverse
4	Nominal	**1.55**	Exp	Earth	Transverse
5	Nominal	**1.73**	Exp	Earth	Transverse
6	**Weak (50%)**	1.08	Exp	Earth	Transverse
7	**Strong (150%)**	1.08	Exp	Earth	Transverse
8	Nominal	1.08	Exp	Earth	**Axial**
9	Nominal	1.08	(3/8)*Exp	Earth	Transverse
10	Nominal	1.08	(3/8)*Exp	**Mars**	Transverse
11	Nominal	1.08	(3/8)*Exp	**Moon**	Transverse
12	Nominal	1.08	(3/8)*Exp	Earth	Axial
13	Nominal	1.08	(3/8)*Exp	**Mars**	Axial
14	Nominal	1.08	(3/8)*Exp	**Moon**	Axial

Hip angles

	Peak flexion (8 cycles)					Peak extension (7 cycles)				
Case	Max (deg)	Min (deg)	Mean (deg)	Std (deg)	p	Max (deg)	Min (deg)	Mean (deg)	Std (deg)	p
2	51.62	49.22	50.65	0.93	-	-35.12	-32.08	-33.29	1.03	-
3	54.81	54.44	54.49	0.13	<0.001	-41.39	-41.24	-41.36	0.06	<0.001
4	51.96	49.50	50.95	0.97	0.547	-32.95	-30.53	-31.91	0.92	0.029
5	52.10	49.62	51.08	0.98	0.398	-32.66	-30.24	-31.62	0.92	0.012
6	56.88	56.45	56.71	0.15	<0.001	-55.58	-38.01	-47.96	5.97	<0.001
7	43.93	41.27	42.71	0.93	<0.001	-30.07	-26.22	-28.26	1.46	<0.001
8	39.30	35.84	37.99	1.29	<0.001	-26.18	-24.13	-25.01	0.70	<0.001
9	25.75	25.62	25.73	0.05	-	-16.02	-15.60	-15.67	0.15	-
10	34.34	33.41	34.12	0.34	<0.001	-18.13	-17.20	-17.40	0.32	<0.001
11	40.56	37.37	39.69	1.15	<0.001	-25.74	-21.23	-22.42	1.52	<0.001
12	18.10	18.00	18.02	0.04	-	-15.07	-15.02	-15.06	0.02	-
13	27.82	27.06	27.31	0.27	<0.001	-23.98	-23.96	-23.97	0.01	<0.001
14	33.23	32.41	32.80	0.30	<0.001	-27.62	-27.27	-27.35	0.11	<0.001

The case numbers down the far left column indicate different configurations. Cases are the SolidWorks Motion Analysis model results for each given input configuration. The three bold horizontal lines separate sections within which statistical analyses were conducted. The nominal case for each section (Case 2, 9 or 12) is at the top and is indicated by the gray shading on the row. Within each section, each Case was compared to the nominal case, with the p-values corresponding to the 2-way T-tests for that comparison, assuming different variances for each Case. Bolded parameters are those that differ between that Case and the section's nominal case.

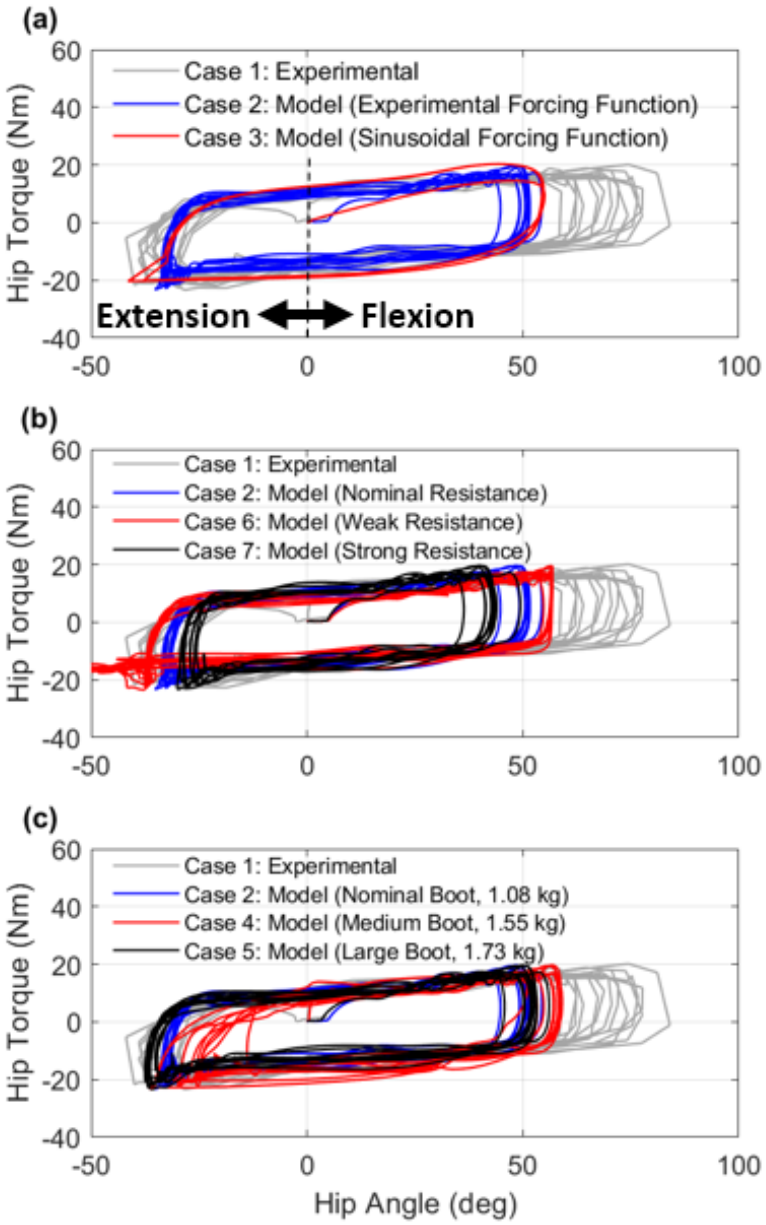


Figure 4. Hysteresis comparisons. (a) Comparison between the experimental data (Case 1), the nominal model (Case 2), and an alternate forcing function (Case 3). The hip torque was applied and the hip angle was measured for the experimental case and estimated for the computational case. (b) Comparison between the nominal model and variable bearing resistances (Cases 6 & 7). (c) Comparison between the nominal model and variable boot mass (Cases 4 & 5). Cases are defined in Tables I and II.

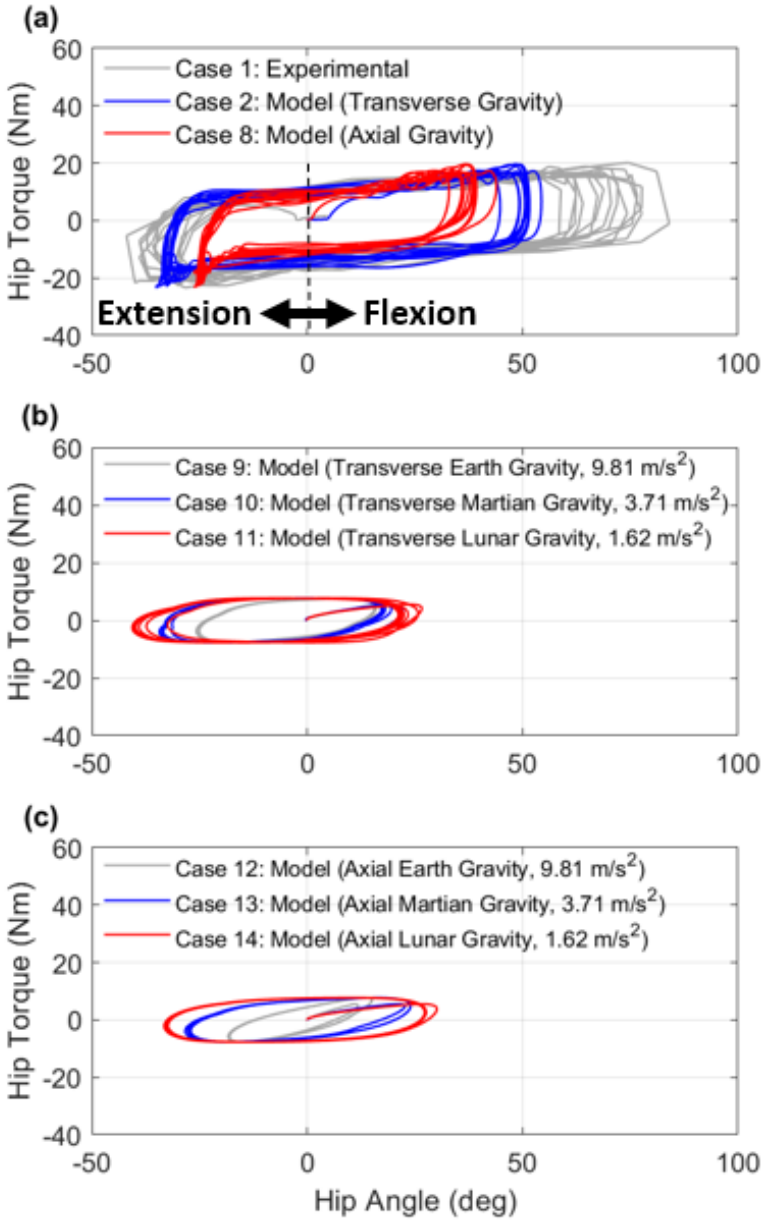


Figure 5. Hysteresis Comparisons with Variable Gravity. (a) Comparison between the experimental data (Case 1), the nominal model with the transversely applied gravity direction (Case 2), and the model with an axially applied gravity direction (Case 8). (b) Comparison between the three gravity levels when gravity is applied in the transverse direction (Cases 9, 10, and 11). For these cases, the forcing function was 3/8ths of the sinusoidal forcing function. (c) Comparison between the three gravity levels when gravity is applied in the axial direction (Cases 12, 13, and 14). For these cases, the forcing function was also 3/8ths of the sinusoidal forcing function.

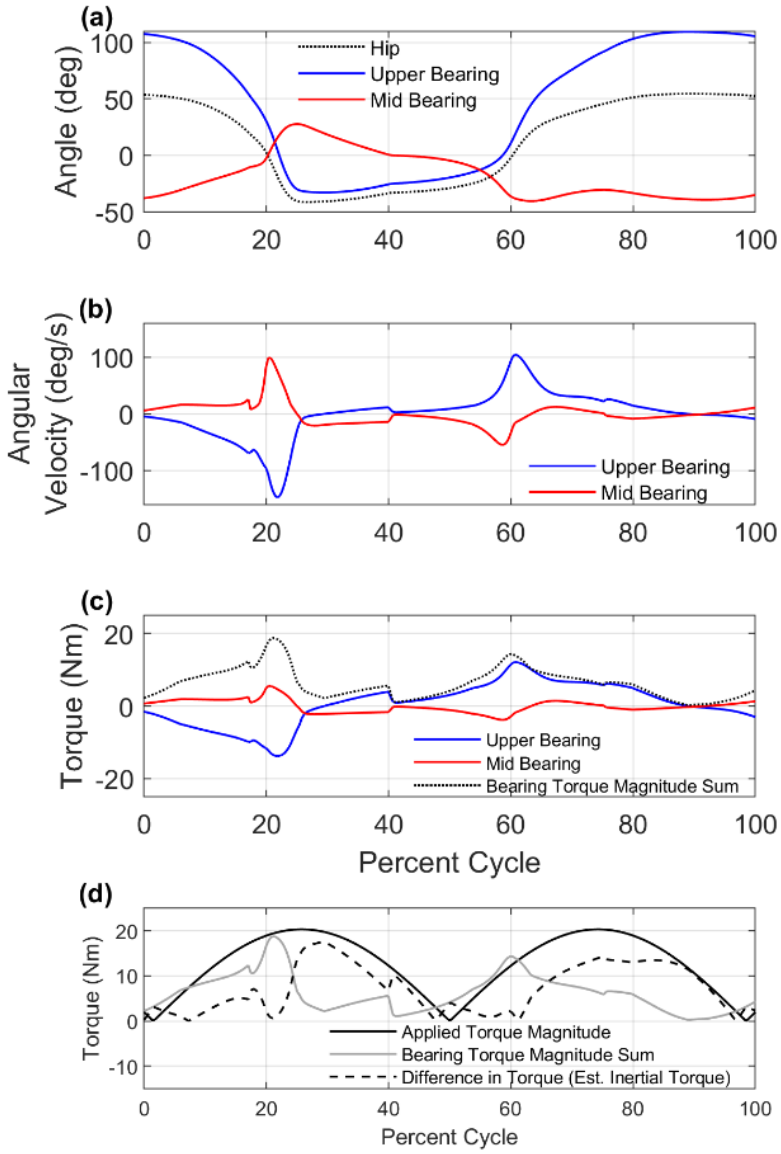


Figure 6. (a) The angular position of each bearing and the hip (in the 2D sagittal plane). (b) The bearing angular velocities. (c) The individual bearing torques and the sum of their absolute values. (d) The total applied torque, the sum of the absolute values of the upper and mid bearing torques, and the difference between these torques as an estimated inertial torque component.

Torque Decomposition

The decomposition of the torques (Fig. 6d) is shown from peak flexion through extension and back to peak flexion. The resistance torque is initially low, when the leg is just past peak flexion. However, the frictional torque increases with angular velocity (Fig. 6b), which increases as the leg returns to the neutral position from 0-20% of the cycle. At the neutral position of the hip (20% cycle), when the bearings are moving at their greatest angular velocity, there is a large resistive component. From 25-50% of the cycle, as the leg extends from neutral to peak extension, the bearing velocities are lower and the applied torque is dominated by the inertial component of moving the mass of the SSA components (inclusive of inertial and gravitational factors). Around 50-60% of the cycle, as the limb moves from maximum extension back towards the neutral position, the torque is applied in the opposite direction and there is a large resistance torque as the bearings increase velocity in the opposite direction. Once past the neutral position (~60% cycle), the bearing velocities (and thus frictional resistances) decrease once more and the inertial component once again dominates until hip is in peak flexion (~90% cycle). Note that at 50% cycle, there is still bearing torque appearing even with zero applied torque since an angular velocity still exists as the suit continues to coast due to the inertial component.

Discussion

Validation

Comparing a complex computational model to a physical system, particularly one that was not designed specifically for the model, is a challenge. The MotionAnalysis model was able to capture the magnitude of the hysteresis and force/angle slopes observed in the experimental data (Fig. 4). As seen in Table I, while peak extension was similar between the model and the experiment ($p=0.194$), peak flexion differed ($p<0.001$). This difference results in the model estimating about 80% of the mean hip angle range compared to the experimental data. There are a few contributing factors that may have led to this discrepancy, including forces the model did not capture and the assumptions made within the model.

One factor that could lead to differences between the experiment and computational model is the absence of forces that were present in the experiment, but un-modeled. For example, there was no data on what force the human test operator applied to the boot when supporting it. The operator may have inadvertently provided additional applied forces encouraging increased flexion and extension, which is consistent with the discrepancy seen in Case 1 and 2. Additionally, the experimental limb moved away from the sagittal plane during the extremes of flexion and extension. It is possible the human test operator was supporting the limb during these intervals, affecting the motion during that time. The geometric constraint in the model provides no supporting force as it moves away from the table. Similarly, there is the possibility that there were additional forces applied at the external forcing point (just distal to the rolling convolute). In videos of the experiment, the operators are seen bending their wrists which changes their forcing direction. In flexion, this change in wrist angle could be significant as the reoriented applied force provides a larger compensatory force against gravity. Essentially, the human operator applied a force of varying direction, but the load cell only recorded the normal force, not the direction of the force or any off-axis forces. Without specific data, the computational model maintained a fixed direction and only forced orthogonally to the HBA. The potential direction changes of the experimental force could have helped compensate against gravity and "lift" the limb further as it moved away from the sagittal plane, possibly affecting the motion during peak flexion by allowing the limb to move farther. These potential differences in applied forces, especially during periods of extreme flexion/extension (when the limb moved away from the sagittal plane), could explain the discrepancies of motion, notably those at peak flexion.

In addition to potential forces which were not captured due to lack of data, there were four potential limitations in the computational model arising from the selected modelling approach: (1) a rigid soft goods section, (2) removal of the rolling convolute pivot, (3) limited mass property documentation, and (4) details of the bearing characterizations. First, in the computational model, a constant knee angle was selected for the soft-goods region. In practice, the knee angle changed (and was not measured) throughout the trial and the overall shape/orientation may change throughout the motion. The biggest change in knee angle, when observing the experimental videos, occurred during the extreme flexion angles. That region was also underestimated by the computational model. The knee flexes close to 90 degrees as the HBA approaches maximum hip flexion, which reduces rotational inertia of the limb and could be a cause of the greater flexion seen in the experiment.

Second, the MKIII HBA has a pivot point at the rolling convolute joint (in addition to its rotation around the leg), at the distal end of the HBA. When operating the suit, the pivot feature provides 7 degrees of adduction and abduction. While the rotation of the rolling convolute was modelled, the pivot point was not represented in the current computational model as it was believed that other boundary conditions, such as the geometric constraint at the boot, restricted this degree of freedom. While these conditions limit motion perpendicular to the sagittal plane (which could limit abduction and adduction), there could still have been motion at the pivot during the experimental trial. The axis of this adduction/abduction pivot changes as bearings rotate when moving from the standard anatomical position to a highly flexed or extended hip angle. Therefore, there may be some unknown effect of that adduction/abduction pivot feature during the experimental analysis that does not manifest during the computational analysis.

Third, the masses in the suit were not documented in the experimental procedures (Valish & Eversley, 2012), so there was no way to determine the exact weights and configurations of the suit that was used the day of testing. Thus, we obtained measures of the masses of the components for a recent suit configuration and assumed these were representative of the past experimental configuration.

Finally, the bearing resistances were based off pooled data and a non-linear regression representing these data. The data used to fit the regression was from a single snapshot in time over an acute 30-hour maintenance schedule, as well as in the lifetime of those bearings. The bearings are sometimes used with a single seal and sometimes with dual seals, which may alter the overall resistance to motion. It was not known whether the bearings had a single or dual seal at the time of the experimental testing for Valish et al. (Valish & Eversley, 2012). It is also unknown if the bearings that were used in the experiment were more or less resistive than the modelled bearings, or if the regression was matched. Figure 4b shows that modelled data from Case 6, with weaker bearing resistances, may more closely resemble the experimental data than the benchmark Case 2, indicating that the resistances may have been weaker during the experimental conditions than when characterized. A related source of potential difference is the lack of characterization of bearing friction under various orientations or loading. The bearing characterization experiments were performed with the bearings parallel to the ground to eliminate the effects of gravity and off-axis loads that could result in internal torques that might affect bearing friction. However, during the experimental study at JSC, the bearings would have had off-axis loading as gravity, the external force, and any supporting forces were not parallel to the bearing axes throughout the motion. This loading could have affected the torque environment inside the bearings, potentially causing different frictional effects.

Sensitivity Analyses

The results from Cases 2 through 14, as shown in Table II and Figures 4 and 5, allow for insight into the effect of various factors on hysteresis and the relationship between hip torque and motion. The dramatic decrease in the standard deviations of peak flexion/extension angles between Case 2, with the experimental forcing function, and Case 3, with the "cleaner" sinusoidal equivalent, indicates that the variation

in these peak angles largely came from the variability in the forcing function. This result is largely unsurprising, but it is worth mentioning because the flexion/extension cycles analyzed were sequential—the limb and its constituent bearings did not return to identical positions between cycles. This finding is true with both sinusoidal and experimental forcing, as can be seen in Figure 4a. Despite this variation in initial state, Case 3 shows a rather small variance in peak flexion/extension angles, indicating that the variance we see in Case 2 stems from the variability in the applied force.

Another interesting result from the sensitivity analysis is the impact of varying frictional versus inertial resistances. Cases 6 and 7 show that changing the bearing resistance impacts both peak flexion and extension, suggesting that the bearing friction resistances play a significant role in the hip motions and required hip torques. Generally, inertial resistances also showed significant impact—modifying the gravity direction (Case 8 vs Case 2) and gravity magnitude (Case 9-11 and 12-14) changed both peak flexion and extension. The purely inertial effects (as opposed to gravity effects) shown in Cases 4 and 5 by adjusting the small boot mass led to a significant change to the peak extension angle, but not in peak flexion.

When gravity is axially applied, the flexion and extension angles both increase as the gravity level decreases (see Fig. 5c). In the axial direction, the externally applied force must counteract the force of gravity, thus reduction of gravity with the same force yields a greater motion. When gravity is transversely applied, the externally applied force only has to push the inertial components of the suit mass and does not counteract the force due to gravity. This difference is observed as the axially applied gravity cases have lower peak hip flexion. The larger peak hip extension angles when gravity is aligned axially is driven by the suit geometry causing the suit to generate out-of-plane motion when moving the hip in extension. The out-of-plane motion is against gravity for the transverse condition, while in the axial condition the motion becomes less aligned with gravity and has less influence.

These results have several implications for operational scenarios. The reduced flexion/extension we see with axial gravity in Case 8 (see Figure 5a) suggest that the hip joint torque results could be underestimated compared to those in operational scenarios. Most uses of spacesuits in planetary environments would feature the astronauts walking, with gravity directed axially. Case 8 (as well as comparing Cases 9-11 to Cases 12-14) indicates that axial gravity decreases the motion generated by a given torque (perhaps as low as 70%) so astronauts could need to provide more effort than anticipated for a given motion. Based on Cases 9-11 and 12-14, the magnitude of this reduction decreases with reduced gravity. Purely inertial factors, such as larger boots or the masses/inertias of other components, could have a smaller impact on required hip torques than bearing resistances (as indicated by the results from Cases 4 and 5). While gravity effects still have a significant impact, this impact is reduced in lower gravity, suggesting these effects could be of less concern in most operational environments for planetary suits (albeit not in training, where most injuries currently are documented)(Stirling et al., 2019). More research is required, but this suggests that attempts to reduce required hip torques for crewmembers should consider the impact of bearing resistances, and how the resistance may be affected by lunar dust and maintenance schedules.

Torque Decomposition

The previous sensitivity analysis investigates how various factors affect the overall suit motion and effect of hip joint torques. This torque decomposition allows for an inspection of the hip joint torques and suit motion over time, particularly regarding the significance of inertial versus frictional components throughout the motion cycles.

In Fig. 6, there is an interplay between the inertia of the SSA components. Nearing peak flexion and extension, there were lower bearing velocities and a greater inertial torque, whereas between the peaks there were considerable torques to overcome the bearing resistances. These data raise questions about how suit occupants adapt into programmed motions under increases in required force/torque, as opposed

to ROM limitations. Shorter et al. (Shorter et al., 2017) showed that a ROM limitation had a compensatory increase in stride length, while an SSA operator was observed to have a reduction in step length (Cullinane et al., 2017b). The resistive, speed-dependent joint torque associated with the spinning bearings and moving suit mass creates additional motion constraints that diminishes the mobility and agility of the operator. The computational model developed in this work enabled the decomposition in the increased required joint torques into its contributing constituents, permitting further understanding of the designed system limitations.

This torque decomposition also allows analysis of potential strategies, within these programmed motions, that could increase the operator's efficiency. There is a strategy, for example, where they could avoid incurring additional applied torques by moving "with the suit" using a strategy at the end of motions (such as strides) where the bearing torques act against the mass/inertial torques to slow the suit components.

Future Work

There are a number of areas of future work targeting extending the model to enable different task assumptions that contributed to the differences in the experimental and computational results. For example, the direction vector of the externally applied force could be variable, as could the boot support force. Both of these adaptions would address previously-mentioned possible sources for discrepancy between the model and the experiment. Future models might also incorporate a knee that can either receive a prescribed kinematic profile (knee angle vs. time) or have defined properties that allow it to behave like a spacesuit knee. Even without recorded data, there is the possibility for studies where these forces and values are approximated and tuned, to investigate hypotheses that these unmodeled forces and uncaptured data account for the discrepancy in the hip joint angle range. The NASA JSC experiment could also be replicated (or modified) with these parameters recorded, to allow for more concrete validation of the current model. Such experiments could also isolate sources of variability, by locking the knee, driving the system with a motor, and either not supporting the boot or using some prismatic joint with a tight constraint.

Even without these additions and extensions, the model in its current state could be used to study other suit motion properties. While not presented in this paper, the model could also be used to examine additional torque relationships, including across joints, or explicitly separating out the effects of gravity. The present work considers a torque decomposition including inertial effects and frictional effects together. A separate method to perform decomposition would be to turn off the bearing resistances, where the resulting required joint torques would be due to inertial effects. Then the mass of the SSA could be turned off to determine the components of the overall torque due to each bearing. This method of selectively turning on and off different resistances and component masses while recalculating the hip angles should be accepted with caution and was not performed here as the recalculation would result in new and distinct kinematic motion profiles.

The bearing resistance expressions used in the model were obtained with only normal forces applied along the axis of rotation (held perpendicular to gravity (Cullinane et al., 2015; Cullinane, Rhodes, & Stirling, 2017a)). However, operationally, the bearings are at alternate angles and experience loads off the axis of rotation. Characterization of off-axis loading is recommended. The bearings will have to be forced by a dynamometer to achieve a range of angular velocities while applying various off-axis loads using cantilevered masses. Bearing resistance estimations could also be adjusted by including the effects of lifecycle, maintenance schedules, and exposure to Lunar or Martian regolith.

It is important to note that in this study, there was no human in the suit. The computational model was compared to an external forcing of the suit. The next steps include using the validated model with a human operator modelled to manipulate the suit internally. A first step could be to use the experimental kinematic data (joint angles) from the JSC study to define the kinematic motion of a motor that drives

the human hip model (HHM) to contact and force the HBA/SSA lower-limb model. This proposed implementation considers the human operator as an open-loop model driving the motion. However, an interesting consideration when including a human is the closed-loop response to human-suit interaction forces or torques. While the inertial effects may dominate during periods of the flexion/extension cycle, the inertial effects may be perceived differently by the human than the frictional forces, or even direct interaction forces. Future efforts should consider the cognitive effects of wearable systems on operational performance and motor selection. There are also opportunities to better understand the physical effects and programmed motions by using the model with the "natural" suit motions generated by an experienced suit operator.

Finally, there is opportunity to use the current model to begin additional trade space analyses. For example, it has been shown that the current bearing architecture does not align with the ROM for natural gait (Cowley et al., 2012). The present model can be used to optimize bearing architectures. The model can also be used to examine strategically placed actuation architectures to reduce the torque required by the human operator during locomotion.

Conclusion

The dynamics model developed in this paper is useful for supplementing experimental suit analyses and can allow for more operationally relevant analyses than are possible experimentally. The dynamics model supported reproduction of the observed hysteretic behavior and was used to perform sensitivity analyses that provided unique insight into the human-suit interactions. Furthermore, the model enabled a decomposition of the underlying torque profiles, showing the relationship between frictional and mass contributions across the motion profile. Future suit evaluations should consider operationally relevant scenarios or couple computational modelling to further explore the design space. The present effort highlights that suit designs should prioritize reducing frictional torques (particularly when used in low-gravity environments), but indicate that strategically minimizing weight also yield benefits.

Funding

This work was supported in part by NASA NCC 9-58, NASA Award NNX15AR20G, and NSTRF NNX15AP51H.

Conflict of Interest Statement

No potential conflict of interest was reported by the authors.

References

Abramov, I., Moiseyev, N., & Stoklitsky, A. (2001). Concept of space suit enclosure for planetary exploration. *SAE Conference*.

Chappell, S. P., Norcross, J. R., J, A. A. F., Bekdash, O. S., Benson, E. A., & Jarvis, S. L. (2017). *Evidence Report : Risk of Injury and Compromised Performance Due to EVA Operations*.

Chullen, C., Mcmann, J., Thomas, K., Kosmo, J., Lewis, C., Wright, R., ... Bitterly, R. (2013). U.S. spacesuit legacy: Maintaining it for the future. *43rd International Conference on Environmental Systems*, 1–23. https://doi.org/10.2514/6.2013-3498

Cowley, M. S., Margerum, S., Hharvill, L., & Rajulu, S. (2012). Model for Predicting the Performance of Planetary Suit Hip Bearing Designs. *International Conference on Applied Human Factors and Ergonomics*. Retrieved from http://ntrs.nasa.gov/search.jsp?R=20130000596

Cullinane, C., Rhodes, R., & Stirling, L. (2015). Mark III Technology Demonstrator Suit: Hip Brief Assembly Bearing Analysis. *International Conference on Environmental Systems*. Bellevue, WA.

Cullinane, C., Rhodes, R., & Stirling, L. (2017a). Mark III Planetary Suit: Follow-up Hip Brief Assembly Bearing Analysis. *International Conference on Environmental Systems*.

Cullinane, C., Rhodes, R., & Stirling, L. (2017b). Mobility and Agility During Locomotion in the Mark III Space Suit. *Aerospace Medicine and Human Performance*, *88*(6), 589–596. https://doi.org/10.3357/AMHP.4650.2017

Flugel, C. W., Kosmo, J. J., & Rayfield, J. R. (1984). *Development of a zero-prebreathe spacesuit*.

Gast, M. A., & Moore, S. K. (2011). A glimpse from the inside of a space suit: What is it really like to train for an EVA? *Acta Astronautica*, *68*(1–2), 316–325. https://doi.org/10.1016/j.actaastro.2010.08.015

Gernhardt, M., Jones, J., Scheuring, R., Abercromby, F., Tuxhorn, J., & Norcross, J. (2009). Risk of Compromised EVA Performance and Crew Health Due to Inadequate EVA Suit Systems. In J. McMurphee & J. Charles (Eds.), *Human Health and Performance Risks of Space Exploration Missions*. NASA SSP-2009-3405.

Graziosi, D., & Ferl, J. G. (1999). *Performance evaluations of an advanced space suit design for International Space Station and Planetary Applications*.

Hoffman, S. J. (2004). Advanced EVA Capabilities: A Study for NASA's Revolutionary Aerospace Systems Concept Program. In *NASA/TP--2004--212068*. Retrieved from http://hdl.handle.net/2060/20040200983

Kosmo, J. J., Spenny, W. E., Gray, R., & Spampinato, P. (1988). *Development of the NASA ZPS Mark III 57.2-kN/m 2 (8.3 psi) Space Suit*.

McKeen, P., & Stirling, L. (2020). Tradespace Exploration of Geometry for a Spacesuit Hip Bearing Assembly. *IEEE Aerospace Conference*. Big Sky, MT.

Newman, D. J., Schmidt, P. B., Rahn, D., Badler, N., & Metaxas, D. (2000). Modeling the Extravehicular Mobility Unit (EMU) Space Suit : Physiological Implications for Extravehicular Activity (EVA). *International Conference on Environmental Systems*. Toulouse, France.

Norcross, J. R., Clowers, K. G., Clark, T., Harvill, L., Morency, R. M., Stroud, L. C., ... Gernhardt, M. L. (2010). Metabolic costs and biomechanics of inclined ambulation and exploration tasks in a planetary suit. *NASA Technical Paper*, *216125*.

Opperman, R. a., Waldie, J. M. a., Natapoff, A., Newman, D. J., & Jones, J. a. (2010). Probability of Spacesuit-Induced Fingernail Trauma Is Associated with Hand Circumference. *Aviation, Space, and Environmental Medicine*, *81*(10), 907–913. https://doi.org/10.3357/ASEM.2810.2010

Scheuring, R. A., Jones, J. A., Novak, J. D., Polk, J. D., Gillis, D. B., Schmid, J., ... Davis, J. R. (2008). The Apollo Medical Operations Project: Recommendations to improve crew health and performance for future exploration missions and lunar surface operations. *Acta Astronautica*, *63*(7–10), 980–987. https://doi.org/10.1016/j.actaastro.2007.12.065

Scheuring, R. A., Mathers, C. H., Jones, J. A., & Wear, M. L. (2009). Musculoskeletal injuries and minor trauma in space: incidence and injury mechanisms in U.S. astronauts. *Aviation, Space, and Environmental Medicine*, *80*, 117–124. https://doi.org/10.3357/ASEM.2270.2009

Schmidt, P. B., & Newman, D. J. (2001). Modeling Space Suit Mobility : Applications to Design and Operations. *International Conference on Environmental Systems*. Orlando, FL, USA.

Shorter, K. A., Wu, A., & Kuo, A. D. (2017). The high cost of swing leg circumduction during human walking. *Gait and Posture*, *54*, 265–270. https://doi.org/10.1016/j.gaitpost.2017.03.021

Stirling, L. A., Arezes, P., & Anderson, A. (2019). Implications of Spacesuit Injury Risk for Developing Computational Performance Models. *Aerospace Medicine and Human Performance*, *90*(6), 553–565.

Valish, D., & Eversley, K. (2012). Space Suit Joint Torque Measurement Method Validation. *International Conference on Environmental Systems*, (July), 1–14. https://doi.org/10.2514/6.2012-3532

Wehner, M., Quinlivan, B., Aubin, P. M., Martinez-Villalpando, E., Baumann, M., Stirling, L., ... Walsh, C. (2013). A lightweight soft exosuit for gait assistance. *IEEE International Conference on Robotics and Automation (ICRA)*, 3362–3369.

Wickman, L. A., & Luna, B. (1996). Locomotion while load-carrying in reduced gravities. *Aviation Space and Environmental Medicine*, *67*, 940–946.